Analytical solution to predict laser ablation rate in a graphitic target

R. Marchiori · W. F. Braga · M. B. H. Mantelli ·
A. Lago

Abstract Laser ablation is a process very useful to obtain many kinds of nanoparticles, included single wall carbon nanotubes (SWNTs). The control of the process, with the aim of determining the temperature conditions during ablation, is required to previously determine the formation and dynamic of growth of nanoparticles. An analytical method to predict the ablation rate is a starting point to set up the experimental conditions, to allow the predefinition of the nanoparticles produced with laser ablation. An ablation method using a pulsed Nd:YAG laser was carried out to ablate a target of graphite, which was irradiated with a laser energy density of 10 J/cm^2 at a temperature of 1,273 K under a controlled atmosphere of Ar. The ablation rate and the heat conduction in the target were studied through an appropriate heat balance method that offers an analytical solution and seems to be very appropriate to describe the ablation conditions. The predictions of ablation rate are in very good agreement with the experimental data.

List of symbols

L	Characteristic length (m)
T_A	Ablation temperature (T)
T_0	Initial temperature (T)
α	Thermal diffusivity (m^2/s)
n	Function degree
δ_P	Dimensionless heat penetration depth
δ_A	Dimensionless ablation depth
u	Dimensionless relative depth ($\delta_P - \delta_A$)
Q_F	Dimensionless heat flux ($Lq''/k(T_A - T_0)$)
v	Inverse Stefan number ($\lambda/C_P(T_A - T_0)$)
θ	Dimensionless temperature ($T - T_0)/(T_A - T_0)$
τ	Dimensionless time ($\alpha t/L^2$)
x	Dimensionless length (X/L)
t	Time (s)
X	Length (m)
λ	Heat of ablation (KJ/kg K)
k	Thermal conductivity (W/m K)

R. Marchiori (✉) · A. Lago
LabMat, Depto de Engenharia Mecânica, Universidade Federal
de Santa Catarina, Campus Universitário, 88040-900
Florianópolis, SC, Brazil
e-mail: robym_67@yahoo.com

W. F. Braga · M. B. H. Mantelli
Lepten/Labtucal, Depto de Engenharia Mecânica, Universidade
Federal de Santa Catarina, Campus Universitário, 88040-900
Florianópolis, SC, Brazil

Introduction

Single Wall Carbon Nanotubes (SWCNTs) can be produced by Laser ablation process by focusing a laser beam at the surface of a graphite target. The produced carbon plasma will condense in form of several different nanoparticles, including SWCNT. When the carbon plasma is allowed to cool in appropriate conditions, the production of SWCNT will be enhanced. Thus, the study of the ablation rate of the target provides important information to tune the process. The heat conduction during ablation is inherently nonlinear and involves a moving boundary inside the target that is not known a priori. According to Chung [1] and Zien [2], the exact analytical solution for transient heat transfer in a solid undertaking ablation is very difficult and practically non-existent. Numerical and approximate analytical solutions have been made available at some conditions and they necessarily require considerable numerical computation,

even if a simplified model of the problem is used in the study.

This work makes use of the heat balance integral method (HBIM) [3] to get a closed form, approximate, analytical solution to obtain ablation rate of a graphitic target with time-variable heat flux.

Literature review

Laser ablation (LA) has been used to obtain SWCNTs with high purity (generally larger than 70% [4, 5]) and little dispersion in diameter of the nanotubes. By adjusting the laser beam parameters, such pulse length, energy it is possible to control in some extend the geometrical, mechanical, and electrical properties of the carbon nano-tubes [6]. These possibilities make LA an interesting process to perform a controlled synthesis of SWNTs.

Many investigations were made to study thermal dynamics during laser ablation, as function of the various parameters of laser [7–9]: the fluence [10–16], the wave-length of laser [14, 17–19], and the pulse duration [12, 16]. In particular, the spectroscopy of the carbon atoms generated by laser ablation of graphite was investigated by Dreyfus and Kelly [20, 21]. These parameters, in combi-nation with the characteristics of the target, determine the ablation rate, the dynamic of vaporization, and heat distribution inside the target.

We studied the thermal behavior of the target during the lasers pulse, as function of the laser pulse length and irradiation in order to obtain the ablation rate. When using a several laser pulses, it is important to investigate the heat conduction occurring at times between two consecutive pulses. Thus, the temporal density of absorbed energy during the pulse, were included in the model.

The first step in this work was to model and simulate the conduction heat transfer, in a graphite target, irradiated by a single laser pulse. This was done by modeling a one-dimensional transient model using MAPLE Software. The obtained ablation rate was compared with the experimental results, obtaining a function $\theta(x,t)$ describing the temper-ature as function of the depth (x) measured from surface of the material and the time (t) in the interval $0 < t < t_p$, where t_p represents the duration of a pulse.

Model of laser heating

Physical modeling

For the present analysis the following simplifications are considered, as suggested by Landau [22]: (1) The heat
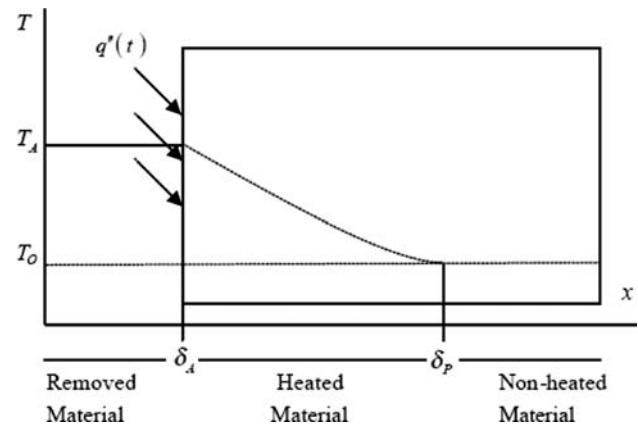
Fig. 1 Schematic drawing of the physical model adopted. At time t, a depth δ_A of the material is ablated and the material is heated up to a depth δ_P

transfer problem is considered one-dimensional. (2) The ablative material properties do not present considerable thermo-physical modifications during the heating process, until it reaches the ablation temperature. All physical–chemical phenomena are assumed to follow a time-variable heat flux. Based on these simplifications the physical model consists of a semi-infinite ablative material which is heated in its surface, by a spatially uniform and time-variable heat source. The laser beam is absorbed in a thin layer at the surface, called heat penetration depth, $\delta_P(t)$, where $\delta_P(0) = 0$. As the time passes, the heating continues until the front face temperature, $T(\delta_A(t), t)$ reaches the ablating temperature level (T_A) and causes the start up of the surface ablation. During the ablation, part of the heat is used to keep the surface at the ablating temperature $(T(\delta_A(t), t) = T_A)$ and the remaining heat is used to change the phase of the ablation material. The phase-change phe-nomenon consumes part of the material. The length of this part is denominated ablation depth, $\delta_A(t)$, where $\delta_A(t_A) = 0$ and t_A is the ablation time, i.e., the time in which $T(\delta_A(t_A), t_A)$ reaches T_A. Figure 1 shows a sche-matic of this physical model.

Mathematical modeling

The 1st pulse

During the first pulse heat conduction inside the target can be described considering the system without heat genera-tion and heat convection. The following transient non-dimensional partial differential heat equation (1) can be used to describe the heat conduction in one dimension. We solved it *at the half-space conditions*, to determine the ablation rate and the heat penetration depth.

$$\frac{\partial \theta}{\partial \tau} = \frac{\partial^2 \theta}{\partial x^2} \tag{1}$$

At Eq. 1, $\theta = (T - T_0)/(T_A - T_0)$ represents the non-dimensional normalized temperature, in which T_0 is the initial temperature and T_A is the ablation reference temperature. In this equation, τ is the Fourier non-dimensional time, defined as $\tau = (\alpha\ t)/L^2$ (non-dimensional Fourier time), where $\alpha = k/\rho \cdot C_P$ is the heat diffusivity, t is the time and L corresponds to an arbitrary length. Also, x is a dimensionless length defined as $x = X/L$, where X is the dimensional length. The parameters k, ρ, and C_P, heat conductivity, density, and heat capacity, respectively, are going to be considered constant in the range of temperature of the process, accordingly with the Landau approximation.

Using the HBIM (heat balance integral method) [23], the Eq. 1 is integrated in x from the solid surface δ_A, that in the pre-ablation step corresponds to $x = 0$, to the heat penetration depth $\delta_P(t)$, obtaining:

$$\int_{\delta_A}^{\delta_P} \frac{\partial \theta}{\partial \tau} dx = \frac{\partial \theta}{\partial x}\bigg|_{x=\delta_P} - \frac{\partial \theta}{\partial x}\bigg|_{x=\delta_A}. \tag{2}$$

As δ_P is a time-dependent variable, the Leibniz rule is used and the Eq. 2 is rearranged as:

$$\frac{\partial}{\partial \tau} \int_{\delta_A}^{\delta_P} \theta dx - \theta|_{x=\delta_P} \frac{\partial \delta_P}{\partial \tau} + \theta|_{x=\delta_A} \frac{\partial \delta_A}{\partial \tau} = \frac{\partial \theta}{\partial x}\bigg|_{x=\delta_P} - \frac{\partial \theta}{\partial x}\bigg|_{x=\delta_A}. \tag{3}$$

At this point, an appropriate function has to be selected as the profile of the temperature distribution inside the material. This function must have a good agreement with the space boundary conditions and must present time-dependent parameters, which are determined using the remaining initial condition. In this article, the following profile is considered:

$$\theta = A \left(\frac{\delta_P - x}{\delta_P - \delta_A} \right)^n \tag{4}$$

where A is the time-dependent parameter used to adjust the adopted temperature profile to the problem solution. Physically, this parameter represents the surface temperature of the material, while n is the exponent of the Eq. 4 and establishes the shape of the temperature profile along the solid, being arbitrarily selected. The best selection of the n value and its implications will be explained latter on this article. The profile represented by Eq. 4 naturally satisfies the boundary conditions given by Eq. 3. Substituting Eq. 4 in Eq. 3 one gets the following ordinary differential equation:

$$\frac{\partial}{\partial \tau} \left(A \frac{(\delta_P - \delta_A)}{(n+1)} \right) + A \frac{\partial \delta_A}{\partial \tau} = \frac{A\ n}{(\delta_P - \delta_A)}. \tag{5}$$

Pre-ablation problem

The following conditions can be considered for the pre-ablation period, that is, $t \leq t_A$, where t_A is the time necessary to the surface to reach the ablation temperature T_A:

$$\begin{aligned}
&\frac{d\delta_A}{d\tau} = 0 \\
&-\frac{\partial \theta}{\partial x} = 0, \quad \text{em } x = \delta_P \\
&\theta = \theta_0 = 0, \quad \text{em } x = \delta_P \\
&-\frac{\partial \theta}{\partial x}\bigg|_{x=\delta_A} = Q_F, \quad \text{em } x = \delta_A = 0
\end{aligned} \tag{6}$$

At the present period, Q_F represents the dimensionless heat flux on side of material that suffers ablation. The conditions in (6) describe the initial situation without moving of surface, where $\delta_A = $ const., arbitrary zero.

The temperature distribution (Eq. 4) is substituted in the heat flux boundary condition (last condition in Eq. 6), obtaining the following equation:

$$\frac{An}{\delta_P}\bigg|_{x=0} = Q_F, \tag{7}$$

Solving for A, one gets:

$$A = \frac{Q_F \delta_P}{n}, \tag{8}$$

Substituting the Eq. 8 in Eq. 5 the following differential equation is obtained:

$$\frac{\partial}{\partial \tau} \left(\frac{Q_F \delta_P^2}{n(n+1)} \right) = Q_F \tag{9}$$

This equation can be easily solved for the heat penetration depth, resulting in:

$$\delta_P = \sqrt{\frac{n(n+1)}{Q_F} \int_0^\tau Q_F d\tau} \tag{10}$$

Considering a constant heat flux, Eqs. 8 and 9 can be rearranged as:

$$\delta_P = \sqrt{n(n+1)(\tau - \tau_0)} \tag{11}$$

and

$$A = \sqrt{\frac{Q^2(n+1)}{n}(\tau - \tau_0)} \tag{12}$$

Considering $A = 1$ and using Eq. 12, one can calculate τ, which is called τ_A, time:

$$\tau_A = \frac{n}{Q^2(n+1)} + \tau_0 \qquad (13)$$

Summarizing, for the prescribed heat flux case, the temperature profile is given by Eq. 4, the surface temperature by Eq. 8 and the heat penetration depth (δ_P) by Eq. 10. Therefore, the only unknown variable is the n parameter.

For the HBIM solutions, one can obtain the following temperature profile, for the prescribed time-constant heat flux problem:

$$\theta = \frac{Q_F \delta_P}{n}\left(1 - \frac{x}{\delta_P}\right)^n; \quad 0 \le x \le \delta_P$$
$$\theta = 0; \quad x \ge \delta_P \qquad (14)$$

Ablation

For the ablation period ($t \ge t_A$), the ablation depth and heat penetration are moving, i.e., $\frac{d\delta_P}{d\tau} > 0$ and $\frac{d\delta_A}{d\tau} > 0$. The following boundary conditions can be considered:

$$-\frac{\partial\theta}{\partial x} = 0 \quad \text{and} \quad \frac{d\delta_P}{\partial\tau} = 0 \quad \text{at } x = \delta_P$$
$$\theta = \theta_0 = 0 \quad \text{at } x = \delta_P$$
$$-\frac{\partial\theta}{\partial x} = Q_F - v\frac{d\delta_A}{d\tau}, \quad \text{at } x = \delta_A = 0 \qquad (15)$$
$$\frac{d\theta}{\partial\tau} = 0 \quad \text{at } x = \delta_A = 0$$
$$\theta = \theta_A = 1 \quad \text{at } x = \delta_A = 0$$

$\frac{d\delta_A}{d\tau}$ is the instantaneous ablation rate, which represents the velocity of consumption of the surface. The temperature distribution (Eq. 4) is substituted in the heat flux boundary conditions (last conditions for $x = \delta_A$ in Eq. 15) obtaining the solution $A = 1$, and solving for $\frac{d\delta_A}{dt}$ one gets, after some manipulation:

$$\frac{d\delta_A}{d\tau} = \frac{Q_F}{v} - \frac{n}{v(\delta_P - \delta_A)} \qquad (16)$$

Substituting (16) in (5), one can obtain:

$$\frac{d}{d\tau}\left[\frac{\delta_P - \delta_A}{(n+1)}\right] + \frac{Q_F}{v} - \frac{n}{v(\delta_P - \delta_A)} = \frac{n}{(\delta_P - \delta_A)}. \qquad (17)$$

Defining u as the relative distance between the heat penetration front and the ablation front, i.e., $u = \delta_P - \delta_A$, Eq. 17 can be rearranged as:

$$\frac{du}{d\tau} = \frac{(n+1)n(v+1)}{(\delta_P - \delta_A)}(n+1)\frac{Q_F}{v} \qquad (18)$$

After some algebra manipulation, introducing u_A as the relative depth at the beginning of ablation, the solution of (18) is:

$$u = \frac{n(v+1)}{Q_F} \cdot \left(\text{LambertW}\left\{\left(\frac{Q_F u_A}{n(v+1)} - 1\right)\right.\right.$$
$$\left.\left. \times \exp\left(\frac{Q_F u_A}{n(v+1)} - 1 - \frac{Q_F(n+1)}{n(v+1)v}\int_{\tau_A}^{\tau} Q_F d\tau\right)\right\} + 1\right) \qquad (19)$$

Substituting Eq. 19 in Eq. 16 and solving for $\delta_A(\tau)$ one obtains:

$$\delta_A = \frac{\int_{\tau_A}^{\tau} Q_F d\tau}{(v+1)} + \frac{u_A}{(n+1)(v+1)} - \frac{n}{Q_F(n+1)}$$
$$\cdot \left(\text{LambertW}\left\{\left(\frac{Q_F u_A}{n(v+1)} - 1\right)\right.\right.$$
$$\left.\left. \times \exp\left(\frac{Q_F u_A}{n(v+1)} - 1 - \frac{Q_F(n+1)}{n(v+1)v}\int_{\tau_A}^{\tau} Q_F d\tau\right)\right\} + 1\right) \qquad (20)$$

From the u definition, using Eqs. 19 and 20 one gets:

$$\delta_P = \frac{\int_{\tau_A}^{\tau} Q_F d\tau}{(v+1)} + \frac{u_A}{(n+1)(v+1)} + \frac{((n+1)(v+1)-1)n}{Q_F(n+1)}$$
$$\cdot \left(\text{LambertW}\left\{\left(\frac{Q_F u_A}{n(v+1)} - 1\right)\right.\right.$$
$$\left.\left. \times \exp\left(\frac{Q_F u_A}{n(v+1)} - 1 - \frac{Q_F(n+1)}{n(v+1)v}\int_{\tau_A}^{\tau} Q_F d\tau\right)\right\} + 1\right) \qquad (21)$$

Considering a constant heat flux and $u_A = \frac{n}{Q_F}$ and from Eqs. 11 and 13, 20 and 21 can be rewritten as:

$$\delta_A = \frac{Q_F(\tau - \tau_A)}{(v+1)} + \frac{n}{Q_F}\frac{1}{(n+1)(v+1)} - \frac{n}{Q_F(n+1)}$$
$$\cdot \left(\text{LambertW}\left\{\left(-\frac{v}{(v+1)}\right)\right.\right.$$
$$\left.\left. \times \exp\left(-\frac{v}{(v+1)} - \frac{Q_F^2(n+1)(\tau - \tau_A)}{n(v+1)v}\right)\right\} + 1\right) \qquad (22)$$

$$\delta_P = \frac{Q_F(\tau - \tau_A)}{(v+1)} + \frac{n}{Q_F}\frac{1}{(n+1)(v+1)}$$
$$+ \frac{n((n+1)(v+1)-1)}{Q_F(n+1)}$$
$$\cdot \left(\text{LambertW}\left\{\left(-\frac{v}{(v+1)}\right)\right.\right.$$
$$\left.\left. \times \exp\left(-\frac{v}{(v+1)} - \frac{Q_F^2(n+1)(\tau - \tau_A)}{n(v+1)v}\right)\right\} + 1\right) \qquad (23)$$

To obtain the ablation rate during the process, i.e., in the several pulses condition, is necessary to evaluate the transient of temperature between the pulses.

Post-ablation

The evaluation of the thermal transient after a pulse is required to obtain the ablation rate, which depends on the cooling dynamic of the material between two adjacent lasers pulses. To evaluate that, is considered the solution of the partial differential heat equation without heat source. This situation is simulated in Maple, adding two pulses with some energy but opposite sign, obtaining the solution of the cooling process without heating, as discussed in the section "Results and discussion".

The heating and cooling profile depend from the parameter n, which determines the heat penetration depth $\delta_P(\tau)$, but has no influence in the ablation rate, as discussed in section below.

Obtaining the parameter n

As introduced before, the n parameter is the exponent of the temperature distribution profile adopted and, generally, is arbitrarily selected. Usually, this profile has an exponential function shape, which satisfies the boundary conditions of the problem, or is a polynomial, that instead, satisfies the boundary conditions, expressed by Eq. 6 [23]. The best selection of the n exponent of temperature profile is based on the study of the optimum parameter for the case of the HBIM method, with $n = 3.66$ as value that presents the minimum error, when compared to classical solution [19], for the surface temperature for the prescribed constant heat flux condition. However, the chose of the value of n have not influence over the ablation rate, which is defined uniquely from the ablation parameters and boundary conditions.

Experimental set-up

Cylindrical graphite targets with diameter of 9.5 and 5 mm in height, were made by pressing graphitic powder with granulometry of 25 μm. The powder was compacted at a pressure of 500 MPa using a double action press. The LA process was carried out using a pulsed Nd:YAG laser operating at wavelength of 1,064 nm and with pulse duration of 200 μs with repetition rate of 10 Hz. The laser beam was focused on the target surface with a 300 μm diameter spot. In Fig. 2 is shown an outline of the experimental apparatus used in the ablation process. The laser pulse duration of 200 μs granted a "soft" vaporization rate without ejecting solid grains of the targets surface.
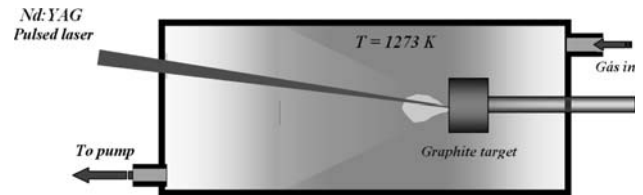
Fig. 2 Schematic of the experimental apparatus. The laser beam was focused at the surface of the target, ablating and generating a plasma of very hot carbon atoms

Test procedure

At the focal point, the laser fluence measured $F_{th} = 10$ J/cm^2 with a repetition rate of 10 pulses per second. The LA process lasted during 1 h at stabilized oven temperature of 1,273 K under the atmosphere of 0.066 MPa of Ar gas with a flow rate of 160 mL/min. During the LA process, the laser beam was scanned uniformly over the surface of the target, preventing the generation of deep holes in the target and resulting in a homogenous vaporization of the surface during ablation. The total amount of ablated material was estimated by carefully weighting the sample after and before the process.

Results and discussion

The parameters used to test the analytical solution process are shown in Table 1. In this table, $P_{ablation}$ represents the pressure of the plasma in the region immediately above the surface, generated from the laser pulse.

Ablation due to single pulse

The heat penetration $\delta_P(\tau)$ and the ablation depth $\delta_A(\tau)$ are showed in Fig. 3, with the relative depths $u(\tau) = \delta_P(\tau) - \delta_A(\tau)$ as a function of time τ during a pulse ($t_p = 200$ μs). In Fig. 3a it can be observed that in the first part of the process, $u(\tau)$ increases, corresponding to a transient period of about 10^{-6} s, in which the material is heating. After this period, the surface reached the temperature of vaporization and the ablation process started, as seen in Fig. 3b. At this moment $u(\tau)$ reached a constant value, i.e., the heat penetration and ablation depths move at the same speed. After the transient period of few microseconds, the constant relative depths $u(\tau)$ means that the material reaches a condition in which the inner surface of the ablated volume material formed a "thermal bath" during the pulse period, being responsible for the heating at the constant distance from the inner surface.

Table 1 Graphite thermophysics properties

Density (g/cm^3)	$P_{ablation}$ (atm)	T of phase change (K) (at 100 atm)	C_p (J/g K)	Absorption coefficient α (cm)$^{-1}$	Conductivity k (W/cm K)
1.9 (experimental)	>100	4800 [20]	$\cong 4.11$ [24] (at the T of phase change)	1.6×10^5 [25]	$5*10^{-2}$ [26]

Fig. 3 a Heat penetration depth $\delta_P(\tau)$, ablation depth $\delta_A(\tau)$, and the relative depth $u(\tau)$ as a function of time, during a pulse ($t_p = 200$ μs). **b** First 0.5 μs of the pulse
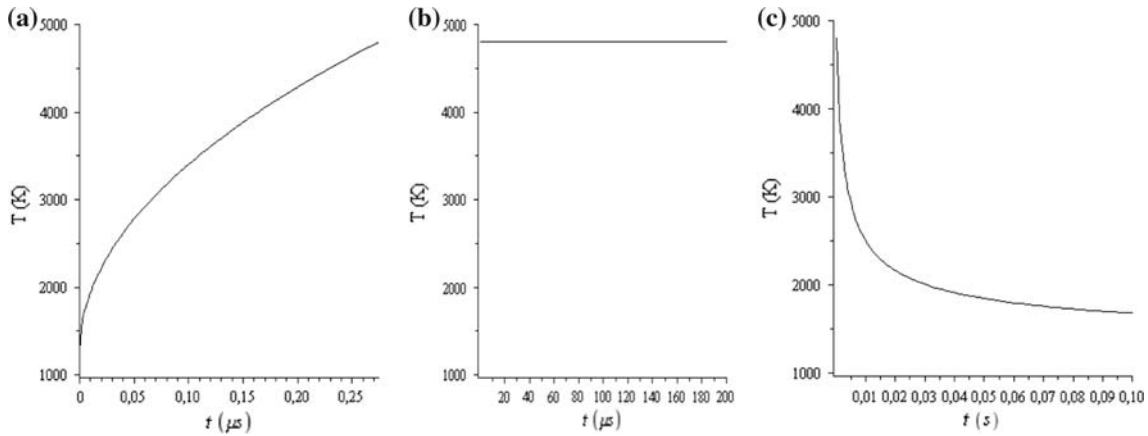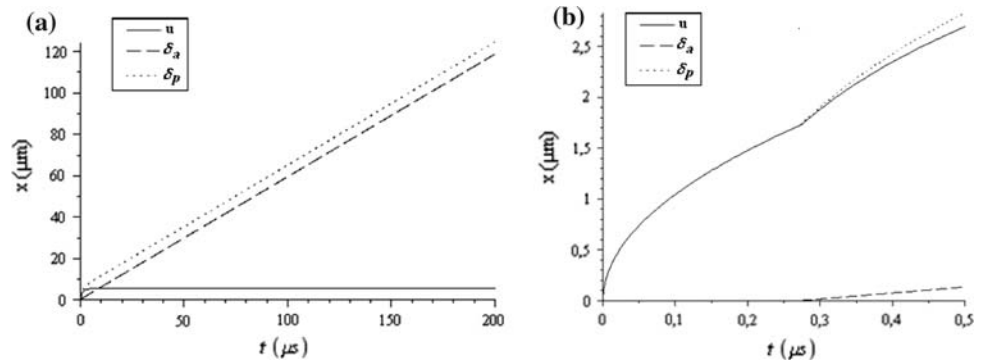

Fig. 4 Heat transient in material during the thermal process. **a** Heating, **b** ablation, and **c** cooling between two pulses

Cooling after pulse ends

After the pulse, the thermal conditions of the surface immediately before the successive pulse are showed in Fig. 4, which visualize the thermal conditions of the surface during the pulse and between two pulses. The Y axis represents the normalized temperature. After heating, the temperature falls very quickly to almost the surrounding temperature, confirming the same starting conditions of surface at all pulses, with a cyclic behavior independent of the number of pulses considered.

Figure 5 presents the temperature distribution inside of the material during one pulse. The region at high temperature represents the part of material that have been removed during the process and the region at low temperature is the material that have not felt the surface heating. It can be observed that there is a very thin heated
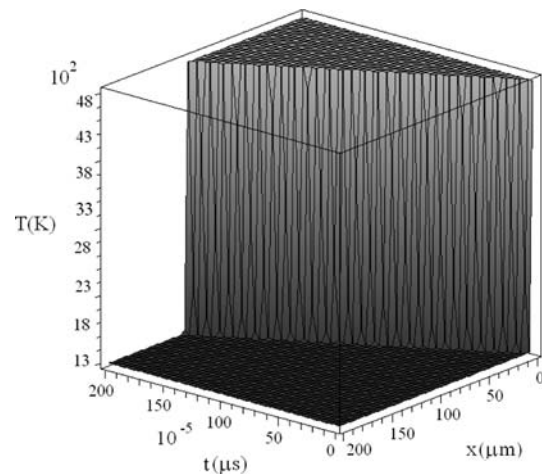
Fig. 5 Temperature distribution for a single pulse (200 μs)
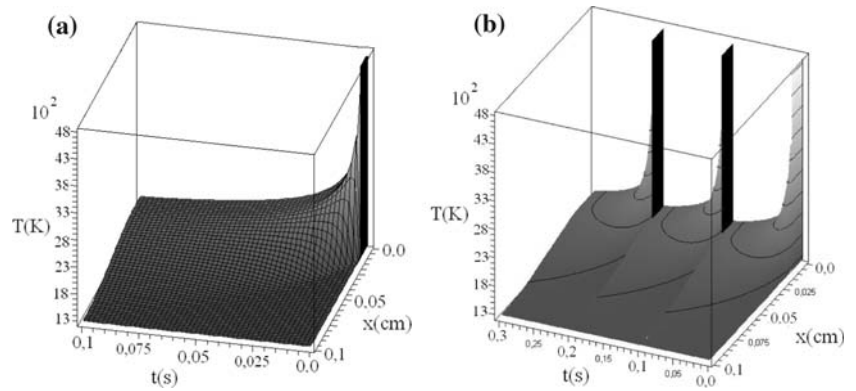
part of the material that is easily cooled during the post-ablation period.

Several pulses

The graphic in Fig. 6a shows the temperature distribution as well as the ablation front $\delta_A(t)$ and the penetration depth $\delta_P(t)$ during the cooling of material between the first and second pulse (200 µs $\leq t \leq$ 0.1 s). Figure 6b indicates the behavior of the several pulses condition; including the heating and the cooling periods, the temperature goes back nearly to the environment temperature, meaning that the surface presents almost the same condition for all pulses. Considering Fig. 3a and b, in the several pulses condition the ablation rate of each pulse is practically the same, because of the very little time (few µs), two orders minor than the pulse period (200 µs), needed to reach the ablation temperature. That condition allows calculating the total ablation amount of material during the several pulses process as a single pulse multiplied by the number of pulses with a final value of almost 0.43 g/h. That value is in the same order of experimental value, of approximately 0.5 g/h, demonstrating that the analytical model used in the simulation was appropriate to be correlated with the experimental conditions.

Conclusions

With the present method is possible to simulate the impact of a single laser pulse on the surface of a target of graphite, obtaining the thermal condition of the surface during the pulse and the transient between two pulses. Consequently, the total ablation of a several pulse process can be estimated with a good agreement with the experimental values.

This description of ablation process allows us to understand the correlation between laser parameters and ablation conditions of the target.

References

1. Chung BTF, Hsiao JS (1985) AIAA J 23:145
2. Zien TF (1978) AIAA J 16:1287
3. Goodman TR (1964) Application of integral methods to transient nonlinear heat transfer. Advances in heat transfer, vol 1. Academic Press, New York, pp 51–122
4. Kingston CT, Jakubek JZ, Dénommée S, Simard B (2004) Carbon 42:1657
5. Maser WK, Benito AM, Martínez MT (2002) Carbon 40:1685
6. Dresselhaus MS, Dresselhaus G, Saito R, Jorio A (2005) Phys Rep 409:47
7. Zhigilei LV, Leveugle E, Garrison BJ, Yingling YG, Zeifman MI (2003) Chem Rev 103:321
8. Brygo F, Semerok A, Oltra R, Weulersse JM, Fomichev S (2006) Appl Surf Sci 252:8314
9. Bogaerts A, Chen Z (2005) Spectrochim Acta B 60:1280
10. Dreiserwerd K, Schürenberg M, Karas M, Hillenkamp F (1995) Int J Mass Spectrom 141:127
11. Miller JC, Haglund RF (1998) Laser ablation and desorption, experimental methods in the physical sciences, vol 30. Academic Press, New York
12. Majaron B, Sustercic D, Lukac M, Skalerič U, Funduk N (1998) Appl Phys B 66:479
13. Bäuerle D (2000) Laser processing and chemistry, 3rd edn. Springer, Berlin
14. Berkenkamp S, Menzel C, Hillenkamp F, Dreiserwerd KJ (2002) Am Soc Mass Spectrom 13:209
15. Lippert T (2004) Polymers and light. Advances in polymer science, vol 168. Springer, Berlin
16. Lewis LJ, Perez D (2009) Appl Surf Sci 10:5101
17. Fabbro R, Fabre E, Amiranoff F, Garban-Labaune G, Virmont J, Weinfeld M, Max CE (1982) Phys Rev A 26:2289
18. Daurelio G, Chita G, Cinquepalmi M (1999) Laser surface cleaning, de-rusting, de-painting and de-oxidizing. Appl Phys A 69:S543
19. Costela A, Garcia-Moreno I, Gomez C, Caballero O, Sastre R (2003) Appl Surf Sci 207:86
20. Dreyfus RW, Kelly R, Walkup RE (1987) Nucl Instr Methods Phys Res B 23(4):557
21. Kelly R, Dreyfus RW (1988) Nucl Instr Methods Phys Res B 32(1–4):341

22. Landau HG (1950) Quart Appl Math 8:81
23. Braga WF, Mantelli MBH, Azevedo JLF (2005) In: AIAA 38th thermophysics conference, Toronto, Ontario
24. Savvatimskiy AI (2005) Carbon 43:1115
25. Besold J, Thielsch R, Matz N, Frenzel C, Born R, Moebius A (1997) Thin Solid Films 293:96
26. Musella M, Ronchi C, Brykin M, Sheindlin M (1998) J Appl Phys 84(51):2530